Set-Based Line-of-Sight (LOS) Path Following with Collision Avoidance for Underactuated Unmanned Surface Vessels under the Influence of Ocean Currents

Signe Moe[1] and Kristin Y. Pettersen[1]

Abstract— **An essential ability of an autonomous unmanned surface vessel (USV) is to follow a predefined path in the presence of unknown ocean currents while avoiding collisions with both stationary and dynamic obstacles. This paper combines recent results for path following and collision avoidance for USVs, resulting in a switched guidance system with a designated path following and a collision avoidance mode. The closed-loop system relies on absolute velocity measurements only, and it is shown that a previously suggested guidance law for collision avoidance guarantees tracking of a safe radius about a dynamic obstacle also under the influence of unknown ocean currents. The guidance law is constructed to ensure collision avoidance while following the International Regulations for Preventing Collisions at Sea (COLREGs). Note that this set-based approach is highly generic and may be applied with any combination of methods for path following and collision avoidance. It is proven that the USV evades the obstacles in a COLREGs compliant manner and converges to the desired path in path following mode. Simulations results validate the theoretical results.**

I. INTRODUCTION

The motion of a marine vehicle is commonly controlled through a guidance, navigation and control (GNC) system [1]. Surface vessels are generally underactuated since they typically lack control inputs in the sideways direction (sway). Thus, the guidance and control system must fulfill the control objectives using only the available actuators in surge (thruster force) and yaw (rudder angle). The control system determines the required thruster force and rudder angle to track the reference states, which are provided by the guidance system. In the case when a surface vessel is given a path following task, the guidance system typically consists of guidance laws for the desired heading and surge velocity that, if tracked, result in the USV converging to and following the desired path. This paper considers a guidance and control system that enables an underactuated USV under the influence of unknown ocean currents to avoid stationary and dynamic obstacles while following a desired path.

A widely used path following method is the line-of-sight (LOS) approach. This approach ensures path following of both straight line [2] and curved paths [3], [4]. It can also be extended using integral effects or ocean current observers to compensate for environmental disturbances, such that path following is achieved also in the presence of ocean currents. In [5] the integral LOS approach is shown to ensure path following of straight line paths.. In [6], a LOS approach is presented which ensures path following of a general path in the presence of unknown ocean currents by guiding the USV to side-slip in such a way that the USV velocity is aligned with the tangent of the path, even if the heading is not. The guidance and control system is based on absolute velocity measurements, and no knowledge of the ocean current magnitude or direction is required. An alternative approach to LOS are backstepping techniques [7]-[9]. Common for the aforementioned path following approaches is that collision avoidance is not considered. This, in addition to the vessel underactuation, results in the need for two guidance system modes: one for path following and one for collision avoidance.

In the marine domain, all surface vessels are required to abide by COLREGs [10]. There exist several methods to achieve collision avoidance, some of which are general and some of which are specific for the nautical case. Potential fields [11], dynamic window [12] and velocity obstacles [10] are widely used collision avoidance approaches. However, use of potential fields may result in oscillations [13], and the dynamic window method assumes that the sideways velocity is zero. Thus, it is unsuitable for USVs, which glide sideways when following curved paths and/or under the influence of ocean currents. The velocity obstacle (VO) approach is not computationally heavy and is straight-forward to comply with COLREGs. However, it is challenging to implement and to combine with existing guidance methods for for instance path following.

The first contribution of this paper is extending recent results for collision avoidance of a USV [14] by proving that a previously suggested LOS-based guidance law for collision avoidance is applicable also when unknown ocean currents are present. In [14], a path following and collision avoidance method is presented that guarantees collision avoidance of both moving and static obstacles while ensuring path following of a straight line path when no ocean currents are present. The results are based on recent work [15], [16] that integrates set-based tasks into the widely used prioritized task kinematic control framework [17], which are then adapted to the underactuation of USVs. The resulting switched guidance system has a path following mode and a collision avoidance mode. A set-based task has a valid range of values, and thus it is possible to define a collision avoidance task as the distance between the USV and an obstacle, where the valid set of

[1]S.Moe and K.Y.Pettersen are with the Center for Autonomous Marine Operations and Systems (NTNU AMOS), at The Department of Engineering Cybernetics, Norwegian University of Science and Technology (NTNU), Trondheim, Norway {signe.moe, kristin.y.pettersen}@itk.ntnu.no

the task has a lower limit of some minimum safe distance. The proposed guidance law for obstacle avoidance, if tracked by the control system, ensures that the USV converges to and follows a circle with constant radius about the obstacle. Furthermore, it is designed specifically to achieve collision avoidance while abiding by the COLREGs. The preliminary results [14] did not suggest a specific guidance law for path following, and only simulations of a straight line path with no influence of currents were presented. The second contribution of this paper is a complete guidance and control system which is applicable to both straight line and curved paths, and is suitable whether ocean currents are present or not. This is achieved by utilizing recent results for path following of USVs under the influence of ocean currents [6]. The resulting guidance and control system relies on absolute measurements only, thereby foregoing the need for expensive sensors to measure relative velocities. The proposed controllers result in exponential tracking of the references, and simulation results validate the proposed method.

This paper has the following structure: The USV model is given in Section II, and the control objectives are defined in Section III. Section IV describes the proposed guidance and control system. The main results are given in Section V, and simulation results and conclusions in Section VI and VII, respectively.

II. VESSEL MODEL

In this section, the 3-DOF maneuvering model and the assumptions on which this is based is presented. For more details on the model, the reader is referred to [1].

A. Model Assumptions

Assumption 1: The motion of the USV is described by 3 degrees of freedom (DOF), that is surge, sway and yaw.

Assumption 2: The USV is port-starboard symmetric.

Assumption 3: The body-fixed coordinate frame b is located at a distance $(x_g^\star, 0)$ from the USV's center of gravity (CG) along the center-line of the USV, where $x_g^\star$ is to be defined later.

Assumption 4: The ocean current in the inertial frame i $\boldsymbol{V}_c \triangleq [V_x, V_y, 0]^T$ is constant, irrotational and bounded. Hence there exists a constant $V_{\max} > 0$ such that $V_{\max} > \sqrt{V_x^2 + V_y^2}$.

B. The Vessel Model

The state of the surface vessel is given by the vector $\boldsymbol{\eta} \triangleq [x, y, \psi]^T$ and describes the position (x, y) and the orientation ψ of the USV with respect to the inertial frame i. The vector $\boldsymbol{\nu} \triangleq [u, v, r]^T$ contains the linear and angular velocities of the USV defined in the body-fixed frame b, where u is the surge velocity, v is the sway velocity and r is the yaw rate. The ocean current velocity in the body frame b, $\boldsymbol{\nu}_c \triangleq [u_c, v_c, 0]^T$, is obtained from $\boldsymbol{\nu}_c = \boldsymbol{R}^T(\psi)\boldsymbol{V}_c$, where $\boldsymbol{R}(\psi)$ is defined as

$$\boldsymbol{R}(\psi) \triangleq \begin{bmatrix} \cos(\psi) & -\sin(\psi) & 0 \\ \sin(\psi) & \cos(\psi) & 0 \\ 0 & 0 & 1 \end{bmatrix}. \tag{1}$$

The relative velocity

$$\boldsymbol{\nu}_r = \begin{bmatrix} u_r \\ v_r \\ r \end{bmatrix} \triangleq \boldsymbol{\nu} - \boldsymbol{\nu}_c = \begin{bmatrix} u \\ v \\ r \end{bmatrix} - \begin{bmatrix} u_c \\ v_c \\ 0 \end{bmatrix} \tag{2}$$

is defined in the body frame b.

The following 3-DOF maneuvering model is considered [1], [18]:

$$\dot{\boldsymbol{\eta}} = \boldsymbol{R}(\psi)\boldsymbol{\nu} \tag{3}$$
$$\boldsymbol{M}_{RB}\dot{\boldsymbol{\nu}} + \boldsymbol{C}_{RB}(\boldsymbol{\nu})\boldsymbol{\nu} = -\boldsymbol{M}_A\dot{\boldsymbol{\nu}}_r - \boldsymbol{C}_A(\boldsymbol{\nu}_r)\boldsymbol{\nu}_r - \boldsymbol{D}(\boldsymbol{\nu}_r)\boldsymbol{\nu}_r + \boldsymbol{B}\boldsymbol{f}$$

The vector $\boldsymbol{f} \triangleq [T, \delta]^T$ contains the control inputs: T is the thruster force and δ is the rudder angle. The matrix $\boldsymbol{M}_{RB} = \boldsymbol{M}_{RB}^T > 0$ is the rigid-body mass and inertia matrix and $\boldsymbol{C}_{RB}$ is the rigid-body Coriolis and centripetal matrix. Similarly, $\boldsymbol{M}_A = \boldsymbol{M}_A^T > 0$ and $\boldsymbol{C}_A$ are mass and Coriolis matrices for hydrodynamic added mass. The strictly positive hydrodynamic matrix is given by $\boldsymbol{D}$ and $\boldsymbol{B} \in \mathbb{R}^{3\times 2}$ is the actuator configuration matrix. The matrices have the following structure:

$$\boldsymbol{M}_x \triangleq \begin{bmatrix} m_{11}^x & 0 & 0 \\ 0 & m_{22}^x & m_{23}^x \\ 0 & m_{23}^x & m_{33}^x \end{bmatrix}, \ \boldsymbol{D}(\boldsymbol{\nu}_r) \triangleq \begin{bmatrix} d_{11} + d_{11}^q u_r & 0 & 0 \\ 0 & d_{22} & d_{23} \\ 0 & d_{32} & d_{33} \end{bmatrix}, \tag{4}$$
$$\boldsymbol{B} \triangleq \begin{bmatrix} b_{11} & 0 \\ 0 & b_{22} \\ 0 & b_{32} \end{bmatrix}, \ \boldsymbol{C}_x(\boldsymbol{z}) \triangleq \begin{bmatrix} 0 & 0 & c_{13} \\ 0 & 0 & m_{11}^x z_1 \\ -c_{13} & -m_{11}^x z_1 & 0 \end{bmatrix},$$

for $x \in \{RB, A\}$, where $c_{13} \triangleq -m_{22}^x z_2 - m_{23}^x z_3$. Ass. 1-3 justify the structure of the matrices $\boldsymbol{M}_x$, $x \in \{RB, A\}$, and $\boldsymbol{D}$ and the structure of $\boldsymbol{C}$ is obtained as described in [1]. Furthermore, the distance $x_g^\star$ from Ass. 3 is chosen so that $\boldsymbol{M}^{-1}\boldsymbol{B}\boldsymbol{f} = [\tau_u, 0, \tau_r]^T$. This point $(x_g^\star, 0)$ exists for all port-starboard symmetric ships [18]. Here, $\boldsymbol{M} = \boldsymbol{M}_{RB} + \boldsymbol{M}_A$.

Remark 1*:* Note that the model (3) does not depend on wave frequency. Hence, the parameters in $\boldsymbol{M}_A$ and $\boldsymbol{D}$ can be considered constant.

Remark 2*:* It is shown in [1] that since the ocean current is constant and irrotational in i, the USV can be described by the 3-DOF maneuvering model in (3).

C. The Model in Component Form

For the control design it is useful to expand (3) into component form:

$$\begin{aligned} \dot{x} &= \cos(\psi)u - \sin(\psi)v \\ \dot{y} &= \sin(\psi)u + \cos(\psi)v \\ \dot{\psi} &= r, \\ \dot{u} &= -\frac{d_{11} + d_{11}^q u}{m_{11}}u + \frac{(m_{22}v + m_{23}r)r}{m_{11}} + \boldsymbol{\phi}_u^T(\psi, r)\boldsymbol{\theta}_u + \boldsymbol{\tau}_u \\ \dot{v} &= X(u_r, u_c)r + Y(u_r)v_r \\ \dot{r} &= F_r(u, v, r) + \boldsymbol{\phi}_r^T(u, v, r, \psi)\boldsymbol{\theta}_r + \tau_r \end{aligned} \tag{5}$$

Here, $m_{ij} \triangleq m_{ij}^{RB} + m_{ij}^A$ and $\boldsymbol{\theta}_u = \boldsymbol{\theta}_r = [V_x, V_y, V_x^2, V_y^2, V_x V_y]^T$. The expressions for $\boldsymbol{\phi}_u^T(\psi, r)$, $X(u_r, u_c)$, $Y(u_r)$, $F_r(u, v, r)$ and $\boldsymbol{\phi}_r^T(u, v, r, \psi)$ are given in App. A.

III. CONTROL OBJECTIVES

In this section, the control objectives considered in this paper are presented: the USV should avoid any obstacles

while abiding by COLREGs, converge to and follow a desired path C, and keep a desired surge velocity along the path. The two first objectives may be in conflict, e.g. if an obstacle is in the middle of the desired path. Hence, should these objectives be contradicting, collision avoidance should and must have the highest priority to guarantee safe passage of the USV and surrounding vehicles.

The path cross-track error y_e is defined as the shortest distance between the USV and any point on the path such that $y_e = 0$ implies that the USV is on the path. The path C is parameterized as a function of θ, and the cross-track error is defined as the orthogonal distance between the USV position (x,y) to the path-tangential reference frame defined by the point $(x_p(\theta), y_p(\theta))$. We assume that the path is an open curve, and Definition 1 [19] guarantees that there exists a unique solution for the cross-track error y_e.

The cross-track error dynamics is defined as

$$\dot{y}_e = -(u\cos(\psi) - v\sin(\psi))\sin(\gamma_p(\theta)) + (u\sin(\psi) + v\cos(\psi))\cos(\gamma_p(\theta)), \tag{6}$$

$$\tag{7}$$

where

$$\gamma_p(\theta) = \operatorname{atan}\left(\frac{y_p'(\theta)}{x_p'(\theta)}\right) \tag{8}$$

is the orientation of the path reference frame in the point (x_p, y_p) [19].

The control objectives of this paper are defined below and presented in prioritized order:

1) The distance between the USV and every obstacle with position $\boldsymbol{p}_{\mathrm{o}}(t)$ should always be greater than or equal to some safe distance R_{o}:
$$|\boldsymbol{p}(t) - \boldsymbol{p}_{\mathrm{o}}(t)| \geq R_{\mathrm{o}} \quad \forall \quad t \geq t_0 \tag{9}$$
2) The USV position should converge to and follow the desired path:
$$\lim_{t\to\infty} y_e(t) = 0 \tag{10}$$
3) The USV surge velocity should converge to some desired, positive velocity:
$$\lim_{t\to\infty} u(t) = u_{\mathrm{des}}(t) \tag{11}$$

IV. THE GUIDANCE AND CONTROL SYSTEM

In this section, the guidance and control system, which consists of guidance laws and controllers, is presented. The guidance system is comprised of separate guidance laws for path following and collision avoidance, as well as an algorithm to switch between these two operational modes of the system.

A. Guidance Laws for Path Following

In path following mode control objective 3 is defined with $u_{\mathrm{des}} = u_{\mathrm{pf}}$, where the desired surge velocity u_{pf} is positive and constant. Moreover, the desired heading in path following mode is denoted ψ_{pf}, where ψ_{pf} is defined as

$$\psi_{\mathrm{pf}}(t) = \gamma_{\mathrm{p}}(\theta) - \underbrace{\arctan\left(\frac{v(t)}{u_{\mathrm{pf}}}\right)}_{\triangleq \beta_{\mathrm{des,pf}}(t)} - \arctan\left(\frac{y_e(t)}{\Delta}\right) \tag{12}$$

and $\Delta > 0$ is a design parameter representing the look-ahead distance. Note that the guidance law (12) is suitable for both straight line and curved paths, and is applicable whether ocean currents are present or not. By calculating the side-slip angle $\beta_{\mathrm{des,pf}}$ based on absolute velocity measurements, the combined effect of path curvature and ocean currents is captured, thereby foregoing the need to estimate the ocean current.

B. Guidance Laws for collision avoidance

In [14], a specific guidance law for USVs is presented to safely avoid obstacles while abiding by COLREGs when no ocean currents are present. This guidance law is given below, and it is proven that it is suitable also for collision avoidance in combination with ocean current compensation. Note that this guidance law is completely independent of the set-based algorithm presented Section IV-D, and that it may be replaced by another collision avoidance method if desired.

In the case of collision avoidance, the goal of the USV is to track a safe radius R_{o} about the obstacle center. If this radius is maintained, a collision will never occur. The position of the obstacle center and its speed are denoted as follows:

$$\boldsymbol{p}_{\mathrm{o}}(t) = \begin{bmatrix} x_{\mathrm{o}}(t) & y_{\mathrm{o}}(t) \end{bmatrix}^T \tag{13}$$

$$U_{\mathrm{o}}(t) = \sqrt{\dot{x}_{\mathrm{o}}(t)^2 + \dot{y}_{\mathrm{o}}(t)^2} \tag{14}$$

Assumption 5: The obstacle speed is upper bounded by $U_{\mathrm{o,max}}$:

$$U_{\mathrm{o}}(t) \leq U_{\mathrm{o,max}} \tag{15}$$

Denote

$$\phi(t) = \arctan\left(\frac{y(t) - y_{\mathrm{o}}(t)}{x(t) - x_{\mathrm{o}}(t)}\right), \tag{16}$$

$$\beta_{\mathrm{o}}(t) = \arctan\left(\frac{\dot{y}_{\mathrm{o}}(t)}{\dot{x}_{\mathrm{o}}(t)}\right), \tag{17}$$

$$V_{\mathrm{o}}(t) = U_{\mathrm{o}}(t)\cos\left(\phi(t) - \beta_{\mathrm{o}}(t)\right), \tag{18}$$

where ϕ and β_{o} are illustrated in Fig. 1. Note that from here on, we omit the argument t for compactness and readability. The physical interpretation of V_{o} is the velocity of the obstacle relative to the USV position, where a negative V_{o} indicates that the obstacle is moving away from the USV and vice versa. It can easily be seen that the maximum value of V_{o}, namely U_{o}, is reached as the obstacle is moving straight towards the current position of the USV (not taking the USV velocity or heading into account).

The desired surge velocity in collision avoidance mode, denoted u_{oa}, is constant and positive.

Assumption 6: It is assumed that the obstacle speed is lower than the desired surge velocity, i.e.

$$u_{\mathrm{oa}} > U_{\mathrm{o,max}}. \tag{19}$$

Remark 3: This is a natural assumption, as it is necessary for collision avoidance to require that the USV moves sufficiently fast to avoid the obstacle by moving around it. Furthermore, Ass. 5-6 ensure that the term k in the collision avoidance heading guidance law (20) is real.

The following guidance law for heading in collision avoidance mode is proposed:

$$\psi_{\text{oa}} = \phi + \lambda\left(\frac{\pi}{2} - \arctan\left(\frac{e+k}{\Delta}\right)\right) - \underbrace{\arctan\left(\frac{v}{u_{\text{oa}}}\right)}_{\triangleq \beta_{\text{des,oa}}}, \tag{20}$$

where $\lambda = \pm 1$ corresponds to clockwise motion and counterclockwise motion, respectively. The parameter λ should be chosen in accordance with COLREGs, see Section IV-C. Furthermore, e is the circle cross-track error, which is defined as

$$e = R_{\text{o}} - \rho = R_{\text{o}} - \sqrt{(x-x_{\text{o}})^2 + (y-y_{\text{o}})^2}, \tag{21}$$

and illustrated in Fig. 1. Moreover, k is defined as

$$k = V_{\text{o}} \frac{-b + \sqrt{b^2 - 4ac}}{2a}, \tag{22}$$

$$a = U_{\text{oa}}^2 - V_{\text{o}}^2 = u_{\text{oa}}^2 + v^2 - V_{\text{o}}^2, \tag{23}$$

$$b = -2V_{\text{o}}e, \tag{24}$$

$$c = -(\Delta^2 + e^2). \tag{25}$$

The parameter k is designed to compensate for the movement of the obstacle. By Ass. 5-6, it is trivial to show that $a > 0$ and $c \leq 0$. Therefore, in the case of a static obstacle, $k = 0$, and for a dynamic obstacle, k has the same sign as V_{o}. Furthermore, the term $\beta_{\text{des,oa}}$ is a side-slip term originally designed to compensate for the curvature of the path, which in the case of a circle is constant $\kappa = R_{\text{o}}^{-1}$. However, this term also compensates for the ocean current effects, similarly to $\beta_{\text{des,pf}}$ in (12): the absolute velocity captures the combined effect of the curvature and ocean current, and allows the USV to converge to and follow the radius R_{o} without knowledge of the ocean current itself. Note that the guidance law (20) requires knowledge of the obstacle's position and velocity, which may be acquired through an automatic identification system (AIS) [20]. Thus, this approach requires no information about the obstacle dimensions or dynamics.

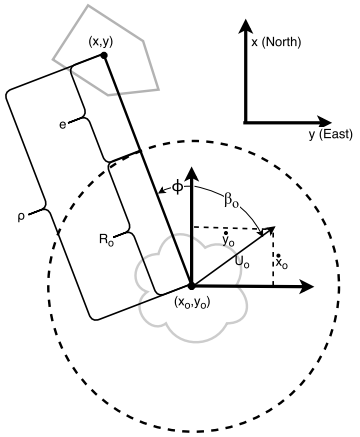

Fig. 1: Illustration of collision avoidance parameters.

Theorem 1. *Given Ass. 5-6, if the guidance laws $u_{\text{des}} = u_{oa}$ and $\psi_{\text{des}} = \psi_{oa}$ are satisfied, the cross-track error e will asymptotically converge to zero and the USV (5) will track the radius R_o about the obstacle center $\boldsymbol{p}_o(t)$.*

Proof. See App. B. □

C. Choosing λ

In (20), the parameter $\lambda = \pm 1$ determines the USV direction of motion about an obstacle, i.e. clockwise or counterclockwise, respectively. COLREGs define the proper direction to the various collision avoidance scenarios: overtaking, crossing from right, head-on and crossing from left [10].

In this paper, λ is chosen according to [14], where the COLREGs situation is determined based on the angle between the fore of the obstacle and the USV. Note that this parameter does not change as the USV circumvents the obstacle and thereby the before-mentioned angle changes. Therefore, as the set-based algorithm activates collision avoidance mode, the collision avoidance scenario is determined and λ is chosen accordingly. This value for λ is kept until the next time the system enters obstacle mode, see Algorithm 1.

D. Set-Based Guidance

The two modes of the system are path following and collision avoidance. In [14] a set-based control approach is presented as a well-defined and deterministic method to switch between these modes. This control approach is given below. Note that this method can be applied with any combination of approaches for path following and collision avoidance. Thus it is not limited to the collision avoidance and path following approaches presented in the previous subsections.

The set-based task σ is defined as the distance between the obstacle center and the USV, which is given by ρ in (21):

$$\sigma = \rho = \sqrt{(x-x_{\text{o}})^2 + (y-y_{\text{o}})^2} \tag{26}$$

It is convenient to rewrite this into polar coordinates to find the expression for the task derivative:

$$x - x_{\text{o}} = \rho\cos(\phi) \tag{27}$$

$$y - y_{\text{o}} = \rho\sin(\phi), \tag{28}$$

where ϕ is defined in (16). Thus,

$$\begin{aligned}\dot{\sigma} &= \frac{2(x-x_{\text{o}})(\dot{x}-\dot{x}_{\text{o}}) + 2(y-y_{\text{o}})(\dot{y}-\dot{y}_{\text{o}})}{2\sqrt{(x-x_{\text{o}})^2 + (y-y_{\text{o}})^2}} \\ &= \frac{\rho\cos(\phi)(\dot{x}-\dot{x}_{\text{o}}) + \rho\sin(\phi)(\dot{y}-\dot{y}_{\text{o}})}{\rho} \\ &= u\cos(\phi-\psi) + v\sin(\phi-\psi) - \sqrt{\dot{x}_{\text{o}}^2 + \dot{y}_{\text{o}}^2}\cos\left(\phi - \arctan\left(\frac{\dot{y}_{\text{o}}}{\dot{x}_{\text{o}}}\right)\right) \\ &= U\cos(\phi - \psi - \beta) - V_{\text{o}}, \end{aligned} \tag{29}$$

where the expressions for $\dot{x}$ and $\dot{y}$ are given in (5), $\beta = \arctan(v/u)$ and we have used the trigonometric formula

$$a\cos(x) + b\sin(x) = \sqrt{a^2+b^2}\cos\left(x - \arctan\left(\frac{b}{a}\right)\right). \tag{30}$$

Furthermore, a mode change radius $R_{\text{m}} > R_{\text{o}}$ about the obstacle is defined:

Assumption 7: The radius R_{m} is chosen sufficiently large that if collision avoidance mode is activated, the USV can converge to the radius R_{o} without overshoot. The necessary radius R_{m} is dependent on the velocities and headings of both the USV and obstacle, the look-ahead distance Δ and the maximum turning radius of the USV.

According to the defined control objectives (9)-(10), the desired motion of the USV is to converge to and follow

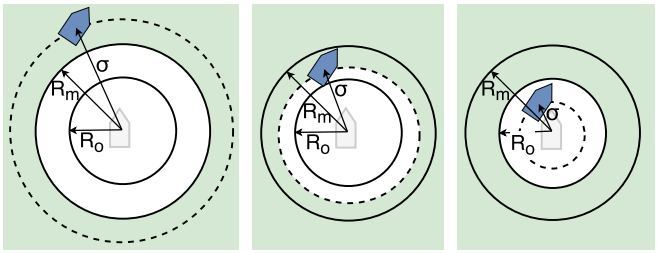

Fig. 2: The set D illustrated in green. For $R_{\mathrm{m}} < \sigma$ (left), path following mode is always active. If $R_{\mathrm{o}} \leq \sigma \leq R_{\mathrm{m}}$ (center), path following is active only if the corresponding $\dot{\sigma} \geq 0$. For $\sigma < R_{\mathrm{o}}$ (right), the USV is outside D and the collision avoidance control objective is violated.

the path C, given that this is possible while maintaining a distance larger than the safe radius R_{o} to any obstacle. Thus, the default mode of the system in path following, and path following should be active as long as the USV is outside the radius R_{m}. However, path following mode may also be active inside R_{m} given that this will increase or maintain the current distance between the obstacle center and the USV, i.e. $\dot{\sigma} \geq 0$ with $u = u_{\mathrm{pf}}$ and $\psi = \psi_{\mathrm{pf}}$. In other words, inside R_{m} collision avoidance is active only as long as the desired behavior in path following mode would result in the USV moving closer to the obstacle. Path following is then reactivated when the path following guidance law will take the USV further away from the obstacle. This switching behavior is described by the *tangent cone* [16]. The tangent cone to the set $D = [\sigma_{\min}, \sigma_{\max}]$ at the point $\sigma \in D$ is defined as

$$T_D(\sigma) = \begin{cases} [\,0, \infty\,) & \sigma = \sigma_{\min} \\ \mathbb{R} & \sigma \in (\sigma_{\min}, \sigma_{\max})\,. \\ (\,-\infty, 0\,] & \sigma = \sigma_{\max} \end{cases} \tag{31}$$

Note that $\dot{\sigma}(t) \in T_D(\sigma(t)) \;\; \forall \;\; t \geq t_0$ implies that $\sigma(t) \in \;\; D \;\; \forall \;\; t \geq t_0$. Thus, we define a set D for the task of collision avoidance, and use this set as a condition for the switched guidance system: the active mode is path following as long as the collision avoidance task σ and the corresponding $\dot{\sigma}$ is in the tangent cone of D. Otherwise, the active mode is collision avoidance. The desired behavior can be captured by defining

$$D = [\min(R_{\mathrm{m}}, \max(\sigma, R_{\mathrm{o}})), \infty), \tag{32}$$

which is illustrated in Fig. 2. As long as $\sigma \in D$, the collision avoidance objective (9) is satisfied.

The switched guidance system is given in Algorithm 1, where line 5 invokes the tangent cone function in_T_C defined in App. C and σ and $\dot{\sigma}$ are defined in (26) and (29) with $u = u_{\mathrm{pf}}$ and $\psi = \psi_{\mathrm{pf}}$.

E. Surge and Yaw Controllers

We define the following error signals:

$$\tilde{u} = u - u_{\mathrm{des}} \tag{33}$$

$$\tilde{\psi} = \psi - \psi_{\mathrm{des}} \tag{34}$$

$$\dot{\tilde{\psi}} = r - \dot{\psi}_{\mathrm{des}} \tag{35}$$

$$\boldsymbol{\xi} = \begin{bmatrix} \tilde{u} & \tilde{\psi} & \dot{\tilde{\psi}} \end{bmatrix}^T \tag{36}$$

```
1  Initialize:
2  last_mode = path_following;
3  λ = −1;
4  while True do
5      a = in_T_C(σ, σ̇, min(R_m, max(σ, R_o)), ∞);
6      if a is True then
7          u_des = u_pf;
8          ψ_des = ψ_pf;
9          mode = path_following;
10     else
11         if last_mode is path_following then
12             choose λ in accordance with COLREGs
13         end
14         u_des = u_oa;
15         ψ_des = ψ_oa(λ);
16         mode = obstacle_avoidance;
17     end
18     last_mode = mode
19 end
```

Algorithm 1: Set-based guidance algorithm.

An adaptive feedback linearizing PD-controller is used to ensure tracking of the desired heading ψ_{des}:

$$\begin{aligned} \tau_r = &-F_r(u,v,r) - \boldsymbol{\phi}_r^T(u,v,r,\psi)\hat{\boldsymbol{\theta}}_r + \ddot{\psi}_{\mathrm{des}} \\ &- (k_\psi + \lambda k_r)\tilde{\psi} - (k_r + \lambda)\dot{\tilde{\psi}} - k_d \mathrm{sign}(\dot{\tilde{\psi}} + \lambda\tilde{\psi}) \end{aligned} \tag{37}$$

$$\dot{\hat{\boldsymbol{\theta}}}_r = \gamma_r \boldsymbol{\phi}_r(u,v,r,\psi)\left(\dot{\tilde{\psi}} + \lambda\tilde{\psi}\right) \tag{38}$$

The gains $k_\psi, k_r, k_d, \lambda, \gamma_r > 0$ are constant and positive, and the function $\mathrm{sign}(x)$ returns 1, 0 and -1 when x is positive, zero or negative, respectively.

Similarly, an adaptive feedback linearizing P-controller is used to ensure tracking of the desired surge velocity u_{des}:

$$\begin{aligned} \tau_u = &-\frac{1}{m_{11}}(m_{22}v + m_{23}r)r + \frac{d_{11}}{m_{11}}u_{\mathrm{des}} - \boldsymbol{\phi}_u^T(\psi,r)\hat{\boldsymbol{\theta}}_u \\ &+ \frac{d_{11}^q}{m_{11}}u^2 + \dot{u}_{\mathrm{des}} - k_u\tilde{u} - k_e \mathrm{sign}(\tilde{u}) \end{aligned} \tag{39}$$

$$\dot{\hat{\boldsymbol{\theta}}}_u = \gamma_u \boldsymbol{\phi}_u(\psi,r)\tilde{u} \tag{40}$$

The constant gains k_u, k_e and γ_u are strictly positive.

The proposed controllers are similar to the controllers in [18], but in this paper the terms $k_d \mathrm{sign}(\dot{\tilde{\psi}} + \lambda\tilde{\psi})$ and $k_e \mathrm{sign}(\tilde{u})$ have been added to increase the robustness of the controller with respect to model uncertainties. Note that the controllers (37) and (39) rely only on absolute velocity measurements, as relative velocities are not available for feedback.

V. MAIN RESULT

In this section, the main result and specific conditions are presented to ensure that the control objectives (9)-(11) are achieved.

Theorem 2. *Given an underactuated USV described by the dynamical system (5). If Ass. 1-7 hold and the state references given by the set-based guidance system in Algorithm 1 are tracked, the control objective (9) is satisfied. As long as the system is in path following mode, the control objective (10) is also fulfilled. Furthermore, the controllers (37)-(38) and (39)-(40) ensure that the surge and*

heading references provided by Algorithm 1 are tracked, and thus the control objective (11) is satisfied.

Proof. In collision avoidance mode, the guidance laws for surge and yaw (20) ensure that the distance between the USV and an obstacle at position $\boldsymbol{p}_o(t)$, denoted ρ, converges to a constant value R_o (Theorem 1). If Ass. 7 is satisfied, this mode is always activated at a distance large enough that $\rho \to R_o$ without overshoot. Given the defined valid set and the tangent cone, path following mode is only reactivated given that it will result in $\dot{\rho} >= 0$. Hence, we can apply the proof in [16] regarding satisfaction of set-based tasks with a valid set defined in (32). Furthermore, the guidance law given in (12), which is active in path following mode, guarantees that the path cross-track error converges asymptotically to zero. Furthermore, the controllers (37)-(38) and (39)-(40) render the equilibrium point $\boldsymbol{\xi} = \mathbf{0}$ uniformly globally exponentially stable. This is proven in [6]. □

VI. SIMULATION RESULTS

In the simulations, the vehicle model is given by (5), with ocean current $V_x = 0.4$ m/s and $V_y = 0.6$ m/s. The simulated vehicle is a HUGIN AUV, produced by Kongsberg Maritime, restricted to movement in the horizontal plane, and the desired surge velocity is chosen to be 4 m/s for both control system modes, i.e. $u_{pf} = u_{oa} = 4$ m/s. The look-ahead distance Δ is chosen as $\Delta = 50$ m. Furthermore, the controller gains are chosen as $k_\psi = 4\text{s}^{-2}$, $k_r = 1.8\text{s}^{-1}$, $\lambda = 2\text{s}^{-1}$, $k_d = 0.18\text{s}^{-2}$, $k_u = 1.5\text{s}^{-1}$ and $k_e = 0.18\text{ms}^{-2}$. The dimensionless adaptive gains are chosen as $\gamma_u = \gamma_r = 1$. Note that to avoid chattering about the equilibrium point, in the simulations the discontinuous term $\text{sign}(z)$ in the controllers (37) and (39) has been replaced by the continuous function $\tanh(10z)$. Finally, a smoothing function has been implemented. This function ensures a smooth transition in the desired heading and surge velocity when switches between the two modes of the system occur, and has been chosen as

$$\alpha(t, t_{\text{switch}}) = \frac{1}{2}\left(\tanh\left(\frac{1}{2}(t - t_{\text{switch}} - 4\right) + 1\right). \tag{41}$$

Two desired paths have been defined and simulated, with a separate set of obstacles in each simulation:

$$C_1 := \begin{cases} x_p(\theta) = & \theta \\ y_p(\theta) = & 30\sin(0.005\theta) \end{cases} \tag{42}$$

$$C_2 := \begin{cases} x_p(\theta) = & 1.2\theta\sin(0.005\theta) \\ y_p(\theta) = & 600\cos(0.005\theta) - 650 \end{cases} \tag{43}$$

Path, obstacle #	R_o [m]	R_m [m]	$\boldsymbol{p}_o(0)$ [m]	$\dot{\boldsymbol{p}}_o(t)$ [m/s]
C_1, 1	100	250	$[500, 75]^T$	$[0, -0.75]^T$
C_1, 2	100	200	$[1600, -70]^T$	$[-0.7, 0]^T$
C_1, 3	75	220	$[2000, -55]^T$	$[0.3, 0]^T$
C_2, 1	130	260	$[200, -500]^T$	$[1, -1]^T$
C_2, 2	200	350	$[-2350, -500]^T$	$[1.5, 0]^T$
C_2, 3	100	250	$[1200, 225]^T$	$[0, -0.75]^T$
C_2, 4	75	220	$[500, -75]^T$	$[-0.3, 0]^T$

TABLE I: Overview of implemented obstacles for path C_1 and C_2: Safe radius R_o, mode change radius R_m, initial position and velocity.

To test robustness, these simulations only consider obstacles that do not abide by COLREGs, i.e. the obstacles do nothing to prevent a collision with the USV. The simulation results are shown in Fig. 3-6. In the simulations, the USV encounters obstacles corresponding to all four COLREGs situations, and successfully avoids them while complying with COLREGs. Furthermore, it converges to and follows the desired path when it is possible to do so without violating the collision avoidance control objective (9) for both paths, see Fig. 5 and 6. Note that the vessel side-slips both in path following and collision avoidance mode. This side-slip both counteract the effects of the ocean current, and the curvature of the path and the safe radius circle around the obstacles. As can be seen in Fig. 3 and 4, the path following cross-track error converges to zero in path following mode, and the controllers (39) and (37) make the USV track the references well. Thus, the defined control objectives (9)-(11) are satisfied.

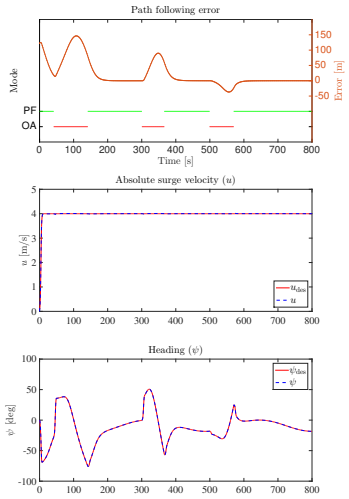

Fig. 3: The path following error and active mode (top) and the desired and actual surge velocity (center) and heading (bottom) for C_1.

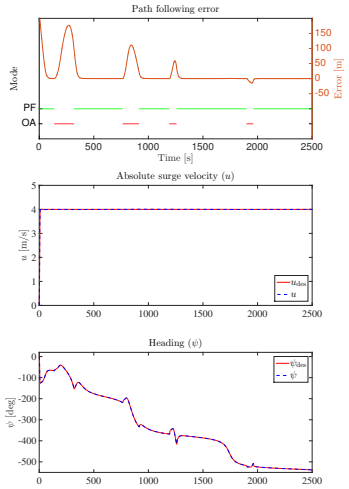

Fig. 4: The path following error and active mode (top) and the desired and actual surge velocity (center) and heading (bottom) for C_2.

VII. CONCLUSIONS

This paper has presented a guidance and control system for a USV that ensures collision avoidance of stationary

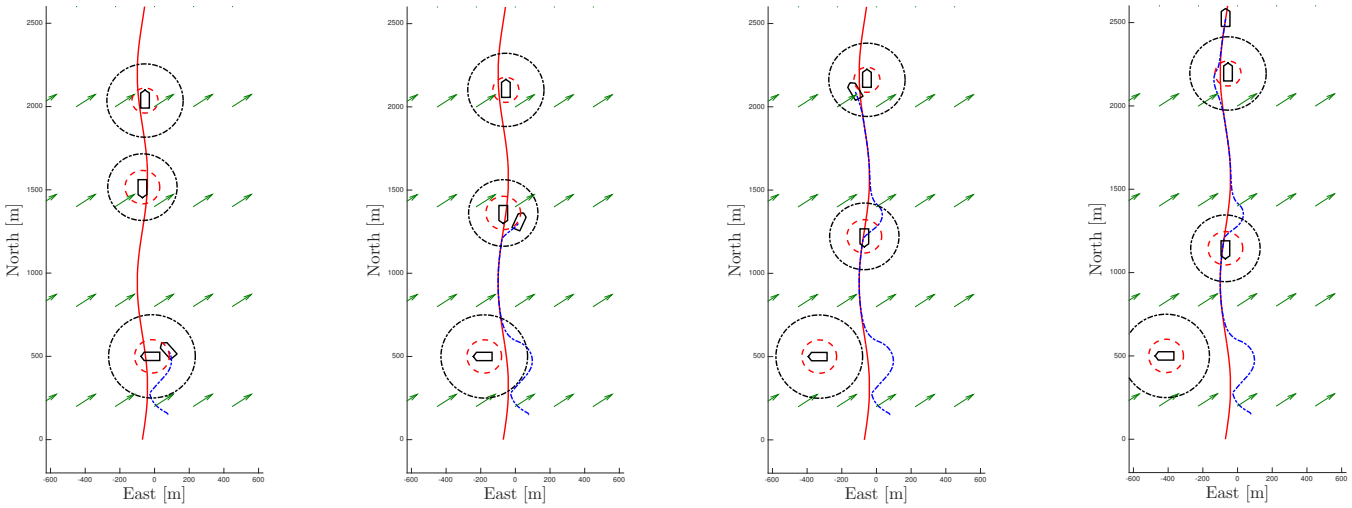

(a) Time = 120 s (b) Time = 340 s (c) Time = 540 s (d) Time = 650 s

Fig. 5: Simulation of with collision avoidance, C_1.

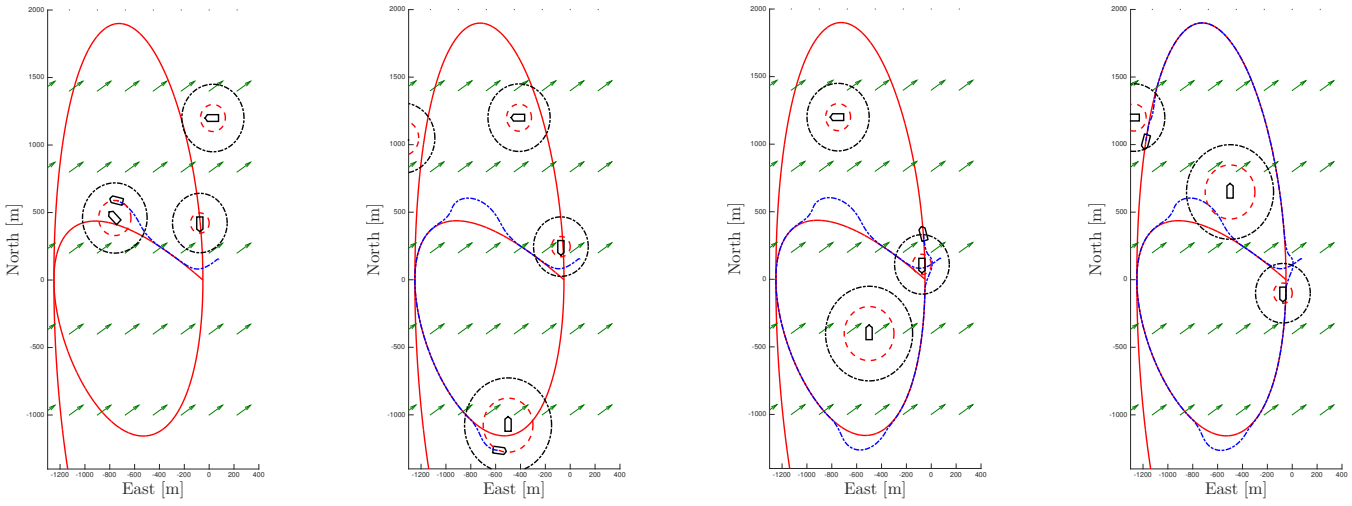

(a) Time = 260 s (b) Time = 850 s (c) Time = 1300 s (d) Time = 2000 s

Fig. 6: Simulation of path following with collision avoidance, C_2. Ocean current in green, desired path in red, USV path in blue and the radii R_o and R_m of the obstacles in dashed red and black, respectively.

and moving obstacles while following a desired path, in the presence of unknown ocean currents. To achieve this, recent results in set-based guidance theory are extended, resulting in a guidance and control system which uses only absolute velocity measurements, and alternates between two defined guidance laws that, if tracked, ensure path following and collision avoidance, respectively, in the presence of ocean currents. Note that this set-based approach is highly generic and may be applied with any combination of methods for path following and collision avoidance. It has been proven that the set-based guidance and control system prevents collisions given that certain, specified assumptions are fulfilled and that the references provided by the guidance system are tracked. Finally, the proposed controllers result in exponential tracking of the references.

Simulation results are presented to validate and illustrate the correctness of the proposed method, where the control objective is to follow two curved paths under the influence of unknown ocean currents. The USV successfully circumvents the obstacles while abiding by COLREGs and converges back to and follows the path when it is safe to do so. Full-scale sea trials will be conducted in the fall of 2017.

APPENDIX A - VESSEL MODEL FUNCTIONS

$$Y(u_r) = \frac{1}{\Gamma}\left(-m_{33}d_{22} + m_{23}d_{32} + m_{23}(m^A_{22} - m^A_{11}u_r)\right) \tag{44}$$

$$X(u_r,u_c) = \frac{1}{\Gamma}\Big(m_{33}(-d_{23} - m_{11}u_r - m^{RB}_{11}u_c) + m_{23}d_{33} + m_{23}(m_{23}u_r + m^{RB}_{23}u_c + m^A_{22}u_c)\Big) \tag{45}$$

$$F_r(u,v,r) = \frac{m_{22}}{\Gamma}\left(-(m_{22}v - m_{23}r)u + m_{11}uv - d_{32}v - d_{33}r\right) - \frac{m_{23}}{\Gamma}\left(-m_{11}ur - d_{22}v - d_{23}r\right) \tag{46}$$

$$\boldsymbol{\phi}_u(\psi,r) = \begin{bmatrix} \frac{d_{11}+2d_{11}^q u}{m_{11}}\cos(\psi) - \frac{m_{11}^A - m_{22}^A}{m_{11}} r\sin(\psi) \\ \frac{d_{11}+2d_{11}^q u}{m_{11}}\sin(\psi) + \frac{m_{11}^A - m_{22}^A}{m_{11}} r\cos(\psi) \\ -d_{11}^q \cos^2(\psi) \\ -d_{11}^q \sin^2(\psi) \\ -2d_{11}^q \cos(\psi)\sin(\psi) \end{bmatrix} \tag{47}$$

Here, $\Gamma = m_{22}m_{33} - m_{23}^2 > 0$. Furthermore, the function $\boldsymbol{\phi}_r(u,v,r,\psi) = [\phi_{r1},...,\phi_{r5}]^T$ is defined by

$$\begin{bmatrix} \phi_{r1} \\ \phi_{r2} \end{bmatrix} = \begin{bmatrix} \cos(\psi) & -\sin(\psi) \\ \sin(\psi) & \cos(\psi) \end{bmatrix} \begin{bmatrix} a_1 \\ a_2 \end{bmatrix} \tag{48}$$

$$\phi_{r3} = -\frac{m_{22}}{\Gamma}(m_{11}^A - m_{22}^A)\sin(\psi)\cos(\psi) \tag{49}$$

$$\phi_{r4} = \frac{m_{22}}{\Gamma}(m_{11}^A - m_{22}^A)\sin(\psi)\cos(\psi) \tag{50}$$

$$\phi_{r5} = \frac{m_{22}}{\Gamma}(m_{11}^A - m_{22}^A)(1-2\sin^2(\psi)), \tag{51}$$

where

$$a_1 = -\frac{m_{22}}{\Gamma}\left((m_{11}^A - m_{22}^A)v + (m_{23}^A - m_{22}^A)r\right) - \frac{m_{23}}{\Gamma}m_{11}^A r \tag{52}$$

$$a_2 = \frac{m_{22}}{\Gamma}\left(d_{32} - (m_{11}^A - m_{22}^A)u\right) - \frac{m_{23}}{\Gamma}d_{22} \tag{53}$$

Remark 4*:* In deriving (44), we have used that $m_{11}^{RB} - m_{22}^{RB} = m - m = 0$, where m is the mass of the vessel [1].

APPENDIX B - PROOF OF THEOREM 1

The error dynamics is given by

$$\dot{e} = \dot{R}_{\mathrm{o}} - \dot{\rho} = -\dot{\rho}, \tag{54}$$

where $\dot{\rho}$ is defined in (29). Under the conditions of Theorem 1, $u = u_{\mathrm{oa}}$ and $\psi = \psi_{\mathrm{oa}}$ (20). It can be shown that this reduces the error dynamics to

$$\dot{e} = -\frac{U_{\mathrm{oa}}}{\sqrt{\Delta^2 + (e+k)^2}}e - \frac{U_{\mathrm{oa}}}{\sqrt{\Delta^2 + (e+k)^2}}k + V_{\mathrm{o}} \tag{55}$$

Furthermore, given the proposed solution of k (22), the sum of the last two terms are identically equal to zero, so

$$\dot{e} = -\frac{U_{\mathrm{oa}}}{\sqrt{\Delta^2 + (e+k)^2}}e. \tag{56}$$

Using the positive definite Lyapunov function $V(e) = 0.5e^2$,

$$\dot{V} = -\frac{U_{\mathrm{oa}}}{\sqrt{\Delta^2 + (e+k)^2}}e^2 \tag{57}$$

is negative definite and the eq.point $e = 0$ of (55) is UGAS [21].

APPENDIX C - THE TANGENT CONE

Input: σ, $\dot{\sigma}$, $\sigma_{\min}$, $\sigma_{\max}$
if $\sigma_{\min} < \sigma < \sigma_{\max}$ **then**
  return True;
else if $\sigma \leq \sigma_{\min}$ *and* $\dot{\sigma} \geq 0$ **OR** $\sigma \geq \sigma_{\max}$ *and* $\dot{\sigma} \leq 0$ **then**
  return True;
else
  return False;
end

Algorithm 2: The boolean function in_T_C.

ACKNOWLEDGMENTS

This work was supported by the Research Council of Norway through the Center of Excellence funding scheme, project number 223254.

REFERENCES

[1] T. I. Fossen, *Handbook of Marine Craft Hydrodynamics and Motion Control*. Wiley, 2011.

[2] S. Oh and J. Sun, "Path following of underactuated marine surface vessels using line-of-sight based model predictive control," *Ocean Engineering*, vol. 37, no. 2-3, pp. 289–295, 2010.

[3] R. Skjetne, U. Jørgensen, and A. R. Teel, "Line-of-sight path-following along regularly parametrized curves solved as a generic maneuvering problem," in *Proc. IEEE Conference on Decision and Control and European Control Conference*, Orlando, FL, USA, 2011, pp. 2467–2474.

[4] E. Børhaug and K. Y. Pettersen, "LOS path following for underactuated underwater vehicle," in *Proc. 7th IFAC Conference on Manoeuvring and Control of Marine Craft*, Lisbon, Portugal, 2006.

[5] W. Caharija, M. Candeloro, K. Y. Pettersen, and A. J. Sørensen, "Relative Velocity Control and Integral LOS for Path Following of Underactuated Surface Vessels," in *Proc. 9th IFAC Conference on Manoeuvring and Control of Marine Craft*, Arenzano, Italy, 2012, pp. 380–385.

[6] S. Moe, K. Y. Pettersen, T. I. Fossen, and J. T. Gravdahl, "Line-of-Sight Curved Path Following for Underactuated USVs and AUVs in the Horizontal Plane under the influence of Ocean Currents," in *Proc. 24th Mediterranean Conference on Control and Automation*, Athens, Greece, 2016.

[7] A. P. Aguiar and J. P. Hespanha, "Trajectory-Tracking and Path-Following of Underactuated Autonomous Vehicles With Parametric Modeling Uncertainty," *IEEE Transactions on Automatic Control*, vol. 52, no. 8, pp. 1362–1379, 2007.

[8] K. D. Do, J. Pan, and Z. P. Jiang, "Robust and adaptive path following for underactuated autonomous underwater vehicles," vol. 31, no. 16, pp. 1967–1997, 2004.

[9] P. Encarnacao and A. Pascoal, "Combined trajectory tracking and path following: an application to the coordinated control of autonomous marine craft," in *Proc. 40th IEEE Conference on Decision and Control*, vol. 1, 2001, pp. 964–969.

[10] Y. Kuwata, M. T. Wolf, D. Zarzhitsky, and T. L. Huntsberger, "Safe Maritime Autonomous Navigation With COLREGS, Using Velocity Obstacles," *IEEE Journal of Oceanic Engineering*, vol. 39, no. 1, pp. 110–119, 2014.

[11] O. Khatib, "Real-time obstacle avoidance for manipulators and mobile robots," in *Proc. IEEE International Conference on Robotics and Automation*, vol. 2, St. Louis, MO, USA, 1985, pp. 500–505.

[12] D. Fox, W. Burgard, and S. Thrun, "The dynamic window approach to collision avoidance," *Robotics Automation Magazine, IEEE*, vol. 4, no. 1, pp. 23–33, 1997.

[13] Y. Koren and J. Borenstein, "Potential field methods and their inherent limitations for mobile robot navigation," in *Proc. IEEE International Conference on Robotics and Automation*, vol. 2, Sacramento, CA, USA, 1991, pp. 1398–1404.

[14] S. Moe and K. Y. Pettersen, "Set-Based Line-of-Sight (LOS) Path Following with Collision Avoidance for Underactuated Unmanned Surface Vessel," in *Proc. 24th Mediterranean Conference on Control and Automation*, Athens, Greece, 2016.

[15] G. Antonelli, S. Moe, and K. Y. Pettersen, "Incorporating Set-based Control within the Singularity-robust Multiple Task-priority Inverse Kinematics," in *Proc. 23rd Mediterranean Conference on Control and Automation*, Torremolinos, Spain, 2015, pp. 1092 – 1097.

[16] S. Moe, G. Antonelli, A. R. Teel, K. Y. Pettersen, and J. Schrimpf, "Set-Based Tasks within the Singularity-Robust Multiple Task-Priority Inverse Kinematics Framework: General Formulation, Stability Analysis, and Experimental Results," *Frontiers in Robotics and AI*, vol. 3, no. 16, pp. 1–18, 2016.

[17] G. Antonelli, "Stability Analysis for Prioritized Closed-Loop Inverse Kinematic Algorithms for Redundant Robotic Systems," *IEEE Transactions on Robotics*, vol. 25, no. 5, pp. 985–994, 2009.

[18] E. Børhaug, A. Pavlov, and K. Y. Pettersen, "Integral LOS control for path following of underactuated marine surface vessels in the presence of constant ocean currents," in *Proc. 47th IEEE Conference on Decision and Control*, Cancun, Mexico, 2008, pp. 4984–4991.

[19] T. I. Fossen and K. Y. Pettersen, "On uniform semiglobal exponential stability (USGES) of proportional line-of-sight guidance laws," *Automatica*, vol. 50, no. 11, pp. 2912–2917, 2014.

[20] Ø. A. G. Loe, "Collision Avoidance for Unmanned Surface Vehicles," Master's thesis, Norwegian University of Science and Technology, 2008.

[21] H. K. Khalil, *Nonlinear systems*. Prentice Hall PTR, 2002.